

Electron spin resonance and exchange paths in the orthorhombic dimer system Sr_2VO_4

J. Deisenhofer,¹ S. Schaile,¹ J. Teyssier,² Zhe Wang,¹ M. Hemmida,¹ H.-A. Krug von Nidda,¹
R. M. Eremina,³ M. V. Eremin,⁴ R. Vienneis,² E. Giannini,² D. van der Marel,⁵ and A. Loidl¹

¹*Experimentalphysik V, Center for Electronic Correlations and Magnetism,
Institute for Physics, Augsburg University, D-86135 Augsburg, Germany*

²*Département de Physique de la Matière Condensée,
Université de Genève, CH-1211 Genève 4, Switzerland*

³*E. K. Zavoisky Physical Technical Institute, 420029 Kazan, Russia*

⁴*Institute for Physics, Kazan (Volga region) Federal University, 430008 Kazan, Russia*

⁵*Département de Physique de la Matière Condensée,
Université de Genève, CH-1211 Genève 4, Switzerland*

(Dated: October 5, 2012)

We report on magnetization and electron spin resonance (ESR) measurements of Sr_2VO_4 with orthorhombic symmetry. In this dimer system the V^{4+} ions are in tetrahedral environment and are coupled by an antiferromagnetic intra-dimer exchange constant $J/k_B \approx 100$ K to form a singlet ground state without any phase transitions between room temperature and 2 K. Based on an extended-Hückel-Tight-Binding analysis we identify the strongest exchange interaction to occur between two inequivalent vanadium sites via two intermediate oxygen ions. The ESR absorption spectra can be well described by a single Lorentzian line with an effective g -factor $g = 1.89$. The temperature dependence of the ESR intensity is well described by a dimer model in agreement with the magnetization data. The temperature dependence of the ESR linewidth can be modeled by a superposition of a linear increase with temperature with a slope $\alpha = 1.35$ Oe/K and a thermally activated behavior with an activation energy $\Delta/k_B = 1418$ K, both of which point to spin-phonon coupling as the dominant relaxation mechanism in this compound.

PACS numbers: 76.30.-v

I. INTRODUCTION

Quantum magnetism is a fascinating research field with a plethora of observed and predicted exotic phenomena such as the Bose-Einstein condensation of magnons¹ or quantum spin-liquids.² In transition-metal oxides where the magnetic ions are in $3d^1$ or $3d^9$ electronic configuration with spin $S = 1/2$ such as, for example, Cu^{2+} cuprates, Ti^{3+} in titanates or V^{4+} in vanadates, the coupling of spin, orbital, and lattice degrees of freedom makes the ground-state properties particularly rich and complex.³⁻⁹

In this study we will focus on orthorhombic Sr_2VO_4 , where the V^{4+} ions are in $3d^1$ configuration and the electron occupies the low-lying e -states in tetrahedral environment as sketched in Fig. 1. The material exhibits orthorhombic symmetry with space group $Pna2_1$ and lattice parameters $a = 14.092(4)$ Å, $b = 5.806(2)$ Å, and $c = 10.106(3)$ Å (see Fig. 1).¹⁰ The orthorhombic distortion can be interpreted in terms of a Jahn-Teller distortion which removes the orbital degeneracy of the V^{4+} ions. No phase transitions have been observed in the temperature range from 4 to 300 K for orthorhombic Sr_2VO_4 . Its susceptibility has been described in terms of a spin-dimer system with a singlet ground state and an antiferromagnetic intra-dimer coupling of about 100 K.¹⁰ However, a clear identification of the superexchange paths corresponding to the magnetic intra-dimer coupling is not available at present, because the superexchange paths between the structural VO_4 units will involve two or more

ligands. Such more complicated super-superexchange (SSE) paths have been found to yield exchange couplings of considerable magnitude and to determine the ground state properties in a large number of compounds.¹¹⁻¹⁴

Here we investigate orthorhombic Sr_2VO_4 by magnetization and electron spin resonance experiments. The exchange paths are analysed by an extended-Hückel-Tight-Binding (EHTB) approach and one dominant exchange path via two intermediate oxygen ions is identified. The ESR intensity confirms the dimer-picture for the susceptibility, the spin-orbit coupling is estimated from the effective g -factor, and the linewidth seems to be governed by a phonon-mediated relaxation mechanism and a thermally activated process.

II. EXPERIMENTAL DETAILS

Ceramic samples were prepared from a $\text{Sr}_4\text{V}_2\text{O}_9$ precursor⁶ by four consecutive reduction and grinding processes at 1100 C in sealed quartz tubes with metallic Zr as an oxygen getter. The samples were characterized by X-ray powder diffraction and showed good agreement with the reported symmetry and lattice parameters.¹⁰ Susceptibility measurements were performed using a SQUID magnetometer (Quantum Design). ESR measurements were performed in a Bruker ELEXSYS E500 CW-spectrometer at X-band frequencies ($\nu \approx 9.47$ GHz) equipped with a continuous He-gas-flow cryostat in the temperature region $4 < T < 300$ K. ESR detects the power P absorbed by the sample from the transverse

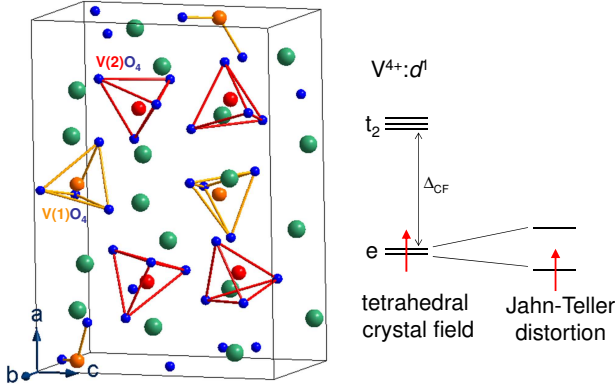


FIG. 1. Left: Unit cell of orthorhombic Sr_2VO_4 with space group $Pna2_1$ (Ref. 10), showing the tetrahedral coordination of the two inequivalent vanadium sites V(1) and V(2). Right: Schematic of the splitting of the V^{4+} d -levels as described in the text.

magnetic microwave field as a function of the static magnetic field H . The signal-to-noise ratio of the spectra is improved by recording the derivative dP/dH using lock-in technique with field modulation.

III. EXPERIMENTAL RESULTS AND DISCUSSION

A. Magnetic Susceptibility

Let us now consider the susceptibility of Sr_2VO_4 as shown in Fig. 2. This system has been described previ-

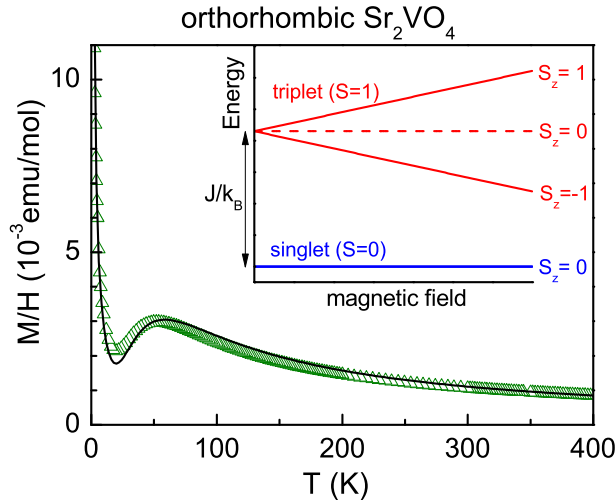


FIG. 2. Temperature dependence of the magnetic susceptibility M/H for orthorhombic Sr_2VO_4 measured in a magnetic field of $\mu_0 H = 0.1$ T. The solid line is a fit using Eq. (1). The inset shows the corresponding energy level scheme of a spin dimer with antiferromagnetic exchange coupling J as a function of the applied field H .

ously as a system of antiferromagnetically coupled spin-dimers with a singlet ground state.¹⁰ To analyze the susceptibility $\chi = M/H$ determined from the magnetization M divided by the applied magnetic field H in the entire temperature range we use

$$\chi = \chi_0 + \chi_C + \chi_{BB}, \quad (1)$$

with a Curie contribution $\chi_C = C/T$ due to unbound spins and magnetic impurities and a constant contribution χ_0 , and the dimer susceptibility χ_{BB} as derived by Bleaney and Bowers:¹⁵

$$\chi_{BB}(T) = \frac{Ng^2\mu_B^2}{k_B T} [3 + \exp(J/k_B T)]^{-1}. \quad (2)$$

Here J denotes the intradimer exchange coupling, g is the effective g -factor of the vanadium ions, and μ_B is the Bohr magneton. The g -factor was fixed to the experimental value $g = 1.89$ observed in the ESR measurements (see below). The obtained fit parameters are $J = 104$ K, $\chi_0 = 1 \cdot 10^{-4}$ emu/mol, which is of the typical order of magnitude for a diamagnetic contribution, and $C = 0.028$ emuK/mol, corresponding to about 7% of unpaired spins. The value for the intradimer exchange $J = 104$ K is in agreement with literature¹⁰ and corresponds nicely to a magnetic excitation peaked at 8.6 meV observed by neutron scattering.¹⁶ From the structural arrangement, however, it is not clear which of the possible exchange paths corresponds to this dominant exchange-coupling constant. Therefore, we performed an extended Hückel-Tight-Binding analysis of the exchange paths which will be discussed in the following.

B. Analysis of the exchange paths

Six distinct exchange paths with exchange couplings J_0 – J_5 and increasing distance between the vanadium ions can be identified in the structure of Sr_2VO_4 (see Fig. 3 and Table II).

The interaction between the magnetic orbitals of two ions in a spin dimer gives rise to two molecular orbitals with an energy split Δe . In the spin-dimer analysis based on EHTB calculations,^{11,17} the strength of an antiferromagnetic exchange interaction between two spin sites is estimated by $J_{AF} = -(\Delta e)^2/U_{eff}$, where U_{eff} is the effective on-site repulsion that is nearly constant for a given compound.

Double- ζ Slater-type orbitals are adopted to describe the atomic s , p , and d orbitals in the EHTB calculations.¹¹ The atomic parameters used for the present EHTB calculations of $(\Delta e)^2$ are summarized in Table I. The parameters of V and O atoms are referred to the previous EHTB calculations on other vanadate compounds,¹⁸ while the rest are taken from the atomic orbital calculations.^{11,19}

As suggested in Ref. 10, the exchange paths between neighboring vanadium atoms could be V–O–O–V or V–

TABLE I. Exponents ζ_i and valence shell ionization potentials H_{ii} of Slater-type orbitals ϕ_i used for extended Hückel tight-binding calculations. H_{ii} are the diagonal matrix elements $\langle \phi_i | H_{eff} | \phi_i \rangle$, where H_{eff} is the effective Hamiltonian. For the calculation of the off-diagonal matrix elements $H_{ij} = \langle \phi_i | H_{eff} | \phi_j \rangle$, the weighted formula as described in Ref. 20 was used. C and C' denote the contraction and diffuse coefficients used in the double- ζ Slater-type orbitals.^{11,18,19}

atom	ϕ_i	H_{ii}	ζ_i	C	$\zeta_{i'}$	C'
V	4s	-8.81	1.697	1.0		
V	4p	-5.52	1.260	1.0		
V	3d	-11.0	5.052	0.3738	2.173	0.7456
Sr	5s	-6.62	1.630	1.0		
Sr	5p	-3.92	1.214	1.0		
O	2s	-32.3	2.688	0.7076	1.675	0.3745
O	2p	-14.8	3.694	0.3322	1.825	0.7448

O–Sr–O–V. According to our calculations, the interactions between second- to sixth-nearest neighboring pairs of V ions are significantly increased, when the strontium atoms are considered in the exchange paths. Therefore, the exchange paths are chosen as V–O–Sr–O–V for J_1 – J_5 (see Fig. 3 (c)–(g)). In contrast, strontium atoms are not considered for the exchange path J_0 .

TABLE II. Values of the V...V distance in Å and $(\Delta e)^2$ associated with the exchange path J_0 – J_5 in Sr_2VO_4

path	V...V	$(\Delta e)^2$	J_i/J_0
J_0	4.090	1370	1.00
J_1	4.682	46	0.03
J_2	4.734	210	0.15
J_3	4.978	55	0.04
J_4	5.381	69	0.05
J_5	5.511	15	0.01

The results of our calculations are summarized in Table II. It shows that the dominant spin-dimer exchange is mediated by the path corresponding to J_0 (see Fig. 3(b)), where the distance between two V ions is shortest. It is interesting that the second strongest exchange is not between the second-nearest-neighbor V ions, but mediated along the path with $J_2 = 0.15J_0$.

C. Electron Spin Resonance

The absorption spectra of Sr_2VO_4 can be described by an exchange-narrowed Lorentzian line shape as shown in the inset of Fig. 4(c). The temperature dependences of the obtained fit parameters are shown in Fig. 4.

The temperature dependence of the ESR intensity I_{ESR} can be well fitted by using Eq. (1) (solid line in Fig. 4(a)) and yields a slightly larger exchange constant $J = 107$ K. The experimental effective g -factor of 1.89 as shown in Fig. 4(b) was used and χ_0 was set to zero,

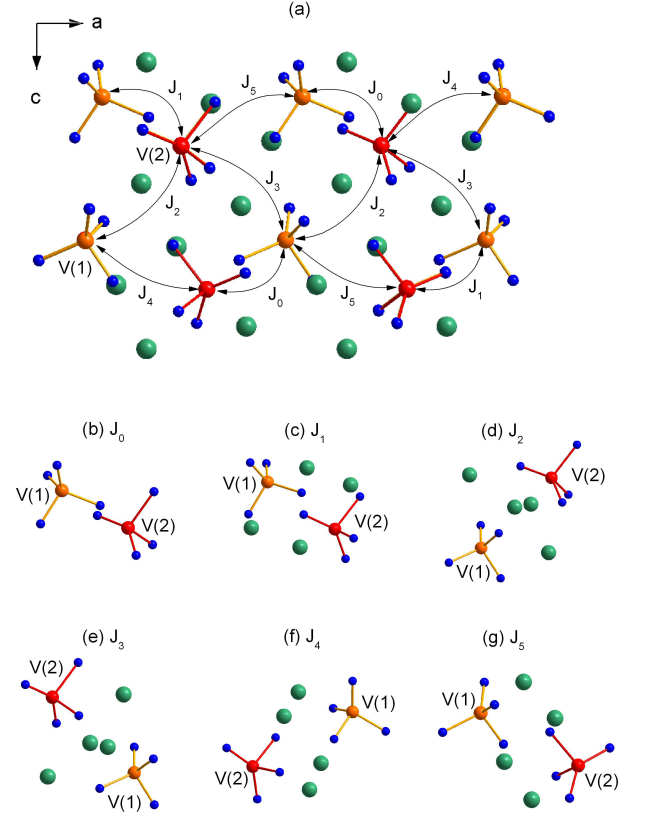


FIG. 3. (Color online) (a) Projection of orthorhombic lattice structure of Sr_2VO_4 with space group $Pna2_1$ on the ac -plane.¹⁰ The exchange paths between neighboring V ions are denoted by the corresponding exchange constants J_0 – J_5 in the sequence of increasing V...V distance. (b)–(g) Spin dimers associated with these exchange paths. The large, middle, and small spheres show Sr, V, and O atoms, respectively. The two crystallographically inequivalent V ions are denoted as V(1) and V(2), respectively.

because it does not contribute to the resonance absorption. These parameters are in agreement with the fit for M/H and show that the resonance absorption originates from magnetic-dipole allowed intra-triplet excitations with $\Delta S_z = \pm 1$ (see inset of Fig. 2). The increase of the g -factor and the decrease of the ESR linewidth below 30 K signal the depopulation of the excited triplet state and the ESR intensity should drop to zero in the ground state. Instead, the intensity increases towards lower temperatures in a Curie-like fashion (solid points) indicating that the resonance signals at lowest temperatures with $g = 1.94$ and $\Delta H = 156$ Oe belong to unpaired paramagnetic ions in the sample.

For the intra-triplet excitations (open symbols) we find an almost temperature independent g -factor $g = 1.89$ between 50 and 150 K. The decrease towards higher temperatures is probably related to the increasing linewidth, which reaches the order of magnitude of the resonance field above 200 K and, hence, imposes a larger uncertainty on the resonance field (or g -factor) as a fitting pa-

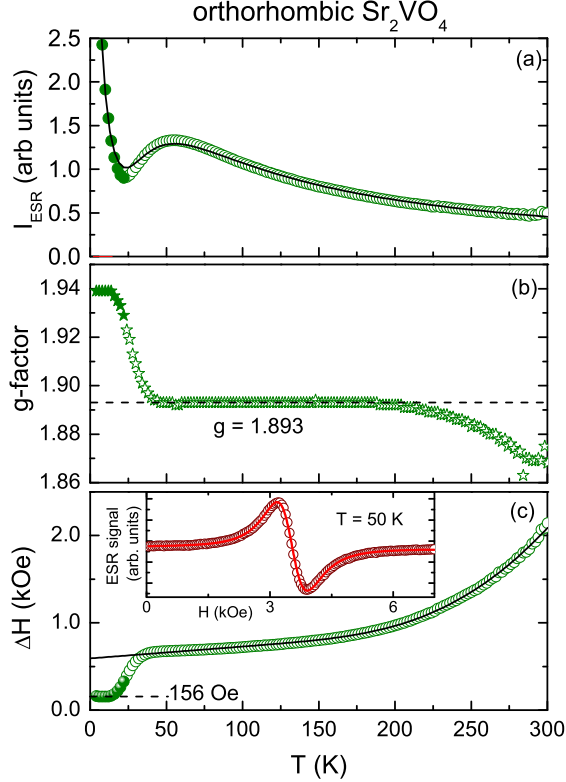


FIG. 4. Temperature dependence of (a) the ESR spin susceptibility together with a fit using Eq. (1), (b) the effective g -factor, and (c) the ESR linewidth in Sr_2VO_4 together with a fit using Eq. (4).

parameter. In first-order perturbation theory the effective g -factor is given by

$$g = 2 - \frac{4\lambda}{\Delta_{CF}}, \quad (3)$$

with the spin-orbit coupling λ and the $e - t_2$ crystal-field splitting parameter Δ_{CF} .²¹ Using $g = 1.89$ and $\Delta_{CF} = 8900 \text{ cm}^{-1}$ as observed by ellipsometry measurements²² we estimate $\lambda = 244 \text{ cm}^{-1}$ (30 meV) in good agreement with the value obtained for V^{4+} ions.^{5,9,21}

The temperature dependence of the ESR linewidth ΔH of the intra-triplet excitations is shown in Fig. 4(c). The linewidth increases monotonously with temperature, between 50 K and 170 K only with a moderate slope but for higher temperatures a strong increase sets in, indicating the presence of at further relaxation mechanisms. The temperature dependence can be well described by

$$\Delta H = \Delta H_0 + \alpha T + A e^{-\frac{\Delta}{k_B T}}, \quad (4)$$

with $\Delta = 1418(19) \text{ K}$, a residual zero-temperature value $\Delta H_0 = 593(5) \text{ Oe}$, $\alpha = 1.35(4) \text{ Oe/K}$, and $A = 1.23(7) \cdot 10^5 \text{ Oe}$.

The linear term can be understood in terms of a spin-phonon relaxation mechanism, where one phonon is involved in the relaxation process.^{21,23,24} The relaxation rate depending on the probabilities for absorption and emission of the phonon will follow a $\coth(\hbar\omega_{ph}/k_B T)$ -behavior which yields a linear behavior for $\hbar\omega_{ph}/k_B T \ll 1$. Hence, any possible source of line-broadening such as a Dzyaloshinsky-Moriya (DM) or symmetric anisotropic exchange interaction, which might be directly modulated by one phonon, could be the origin of the linear contribution.^{21,23–25} We want to mention that we have no indication of the presence of a sizeable static DM interaction. However, there is no center of inversion between the two inequivalent V sites and a static DM contribution within the dimers could arise.

A thermally activated contribution has been observed for several low-dimensional magnets^{26–28} and in the dimer system $\text{Sr}_3\text{Cr}_2\text{O}_8$, where the Cr^{5+} also have an electronic $3d^1$ configuration in a tetrahedral crystal field.²⁹ In the latter compound the value of $\Delta = 388 \text{ K}$ is lying within the phonon frequency range and the contribution was tentatively assigned to stem from a two-phonon Orbach process, where the spin relaxation occurs via an absorption of a phonon to a higher-lying electronic state in the energy range of the phonon continuum. For Sr_2VO_4 the value $\Delta = 1418(19) \text{ K}$ is too high for phonon modes and rules out the presence of an Orbach mechanism. Since all of the mentioned studies deal with Jahn-Teller active ions, another possible origin of such a thermally activated behavior could be the presence of different Jahn-Teller distortions, which are close in energy, e.g. in case of the one-dimensional magnet CuSb_2O_6 (Cu^{2+} with spin 1/2 in octahedral environment) the exponential increase of the linewidth with $\Delta = 1484 \text{ K}$ has been observed on approaching a static-to-dynamic Jahn-Teller transition at 400 K.²⁶ The value of Δ would then correspond to the energy barrier separating the two Jahn-Teller configurations.

IV. SUMMARY

In summary, we investigated orthorhombic Sr_2VO_4 by electron spin resonance measurements and identified the dominating exchange path to occur between two inequivalent vanadium sites via two intermediate oxygen ions using an extended-Hückel-tight binding analysis. The temperature dependence of the ESR intensity and the magnetization reveal a dimerized singlet ground state with an intradimer coupling constant $J/k_B \approx 100 \text{ K}$. The ESR linewidth exhibits an increase with rising temperature which can be understood in terms of a phonon-modulated spin relaxation yielding a linear increase with slope $\alpha = 1.35 \text{ Oe/K}$ and a thermally activated Arrhenius behavior with an activation energy $\Delta/k_B = 1418 \text{ K}$, which might be related to the Jahn-Teller distortion of the system.

ACKNOWLEDGMENTS

We thank D. Vieweg for experimental support and H.-J. Koo and M.-H. Whangbo for fruitful discussions with regard to the EHTB calculation. This work is partially supported by the SNSF through Grant No.

200020-130052 and the National Center of Competence in Research (NCCR) Materials with Novel Electronic Properties-MaNEP and by the DFG via the Collaborative Research Center TRR 80 (Augsburg-Munich) and project DE 1762/2-1.

-
- ¹ T. Giamarchi, C. Rüegg, and O. Tchernyshyov, *Nature Physics* **4**, 198 (2008).
 - ² L. Balents, *Nature (London)* **464**, 199 (2010).
 - ³ Y. Tokura and N. Nagaosa, *Science* **288**, 462 (2000).
 - ⁴ H. D. Zhou, B. S. Conner, L. Balicas, and C. R. Wiebe, *Phys. Rev. Lett.* **99**, 136403 (2007).
 - ⁵ G. Jackeli and G. Khaliullin, *Phys. Rev. Lett.* **103**, 067205 (2009).
 - ⁶ R. Viennois, E. Giannini, J. Teyssier, J. Elia, J. Deisenhofer, and D. van der Marel, *J. Phys.: Conf. Ser.* **200**, 012219 (2010).
 - ⁷ H. D. Zhou, Y. J. Jo, J. Fiore Carpino, G. J. Munoz, C. R. Wiebe, J. G. Cheng, F. Rivadulla, and D. T. Adroja, *Phys. Rev. B* **81**, 212401 (2010).
 - ⁸ J. Teyssier, R. Viennois, E. Giannini, R.M. Eremina, A. Günther, J. Deisenhofer, M.V. Eremin, and D. van der Marel, *Phys. Rev. B* **84**, 205130 (2011).
 - ⁹ M.V. Eremin, J. Deisenhofer, R.M. Eremina, J. Teyssier, D. van der Marel, and A. Loidl, *Phys. Rev. B* **84**, 212407 (2011).
 - ¹⁰ W. Gong, J.E. Greedan, G. Liu, and M. Bjorgvinsson, *J. Sol. State Chem.* **94**, 213 (1991).
 - ¹¹ M.-H. Whangbo, H.-J. Koo, and D.J. Dai, *Solid State Chem.* **176**, 417 (2003); M.-H. Whangbo, D. Dai, and H.-J. Koo, *Solid State Sci.* **7**, 827 (2005).
 - ¹² J. Deisenhofer, R. M. Eremina, A. Pimenov, T. Gavrilova, H. Berger, M. Johnsson, P. Lemmens, H.-A. Krug von Nidda, A. Loidl, K.-S. Lee, and M.-H. Whangbo, *Phys. Rev. B* **74**, 174421 (2006).
 - ¹³ R. M. Eremina, T. P. Gavrilova, A. Günther, Z. Wang, M. Johnsson, H. Berger, H.-A. Krug von Nidda, J. Deisenhofer, and A. Loidl, *Eur. Phys. J. B* **84**, 391 (2011).
 - ¹⁴ Z. Wang, M. Schmidt, Y. Goncharov, Y. Skourski, J. Wosnitza, H. Berger, H.-A. Krug von Nidda, A. Loidl, J. Deisenhofer, *J. Phys. Soc. Jpn.* **80**, 124707 (2011).
 - ¹⁵ B. Bleaney and K.D. Bowers, *Proc. R. Soc. A* **214**, 451 (1952).
 - ¹⁶ S. Toth et al., in preparation.
 - ¹⁷ Our calculations were carried out by employing the SAMOA (structure and molecular orbital analyzer) program package (M.-H. Whangbo *et al.*, North California State University, <http://www.primec.com/products.htm>).
 - ¹⁸ H.-J. Koo, M.-H. Whangbo, P. D. VerNooy, C. C. Toraridi, and W. J. Marshall, *Inorg. Chem.* **41**, 4664 (2002).
 - ¹⁹ E. Clementi and C. Dai, *J. Solid State Chem.* **14**, 177 (1974).
 - ²⁰ J. Ammeter, H.-B. Bürgi, J. Thibault, and R. Hoffmann, *J. Am. Chem. Soc.* **100**, 3686 (1978).
 - ²¹ A. Abragam and B. Bleaney, *Electron Paramagnetic Resonance of Transition Ions* (Oxford, 1970).
 - ²² J. Teyssier et al., in preparation.
 - ²³ M. S. Seehra and T. C. Castner, *Phys. Kondens. Mater.* **7**, 185 (1968).
 - ²⁴ T. G. Castner, Jr. and M. S. Seehra, *Phys. Rev. B* **4**, 38 (1971).
 - ²⁵ A. Zorko, D. Arcon, H. van Tol, L. C. Brunel, and H. Kageyama, *Phys. Rev. B* **69**, 174420 (2004).
 - ²⁶ M. Heinrich, H.-A. Krug von Nidda, A. Krimmel, A. Loidl, R. M. Eremina, A. D. Ineev, B. I. Kochelaev, A. V. Prokofiev, W. Assmus *Phys. Rev. B* **67**, 224418 (2003).
 - ²⁷ D.V. Zakharov, J. Deisenhofer, H.-A. Krug von Nidda, P. Lunkenheimer, J. Hemberger, M. Hoinkis, M. Klemm, M. Sing, R. Claessen, M.V. Eremin, S. Horn, and A. Loidl, *Phys. Rev. B* **73**, 094452 (2006).
 - ²⁸ M.V. Eremin, D.V. Zakharov, H.-A. Krug von Nidda, R.M. Eremina, A. Shuvaev, A. Pimenov, P. Ghigna, J. Deisenhofer, and A. Loidl, *Phys. Rev. Lett.* **101**, 147601 (2008).
 - ²⁹ Z. Wang, M. Schmidt, A. Günther, S. Schaile, N. Pascher, F. Mayr, Y. Goncharov, D.L. Quintero-Castro, A. T. M. N. Islam, B. Lake, H.-A. Krug von Nidda, A. Loidl, and J. Deisenhofer, *Phys. Rev. B* **83**, 201102(R) (2011).